



Numerical Modelling of Trapped Electrons in an Expanding Solar Loop

L. Fletcher¹ and H. S. Hudson²

(1) University of Glasgow
(2) University of California, Berkeley

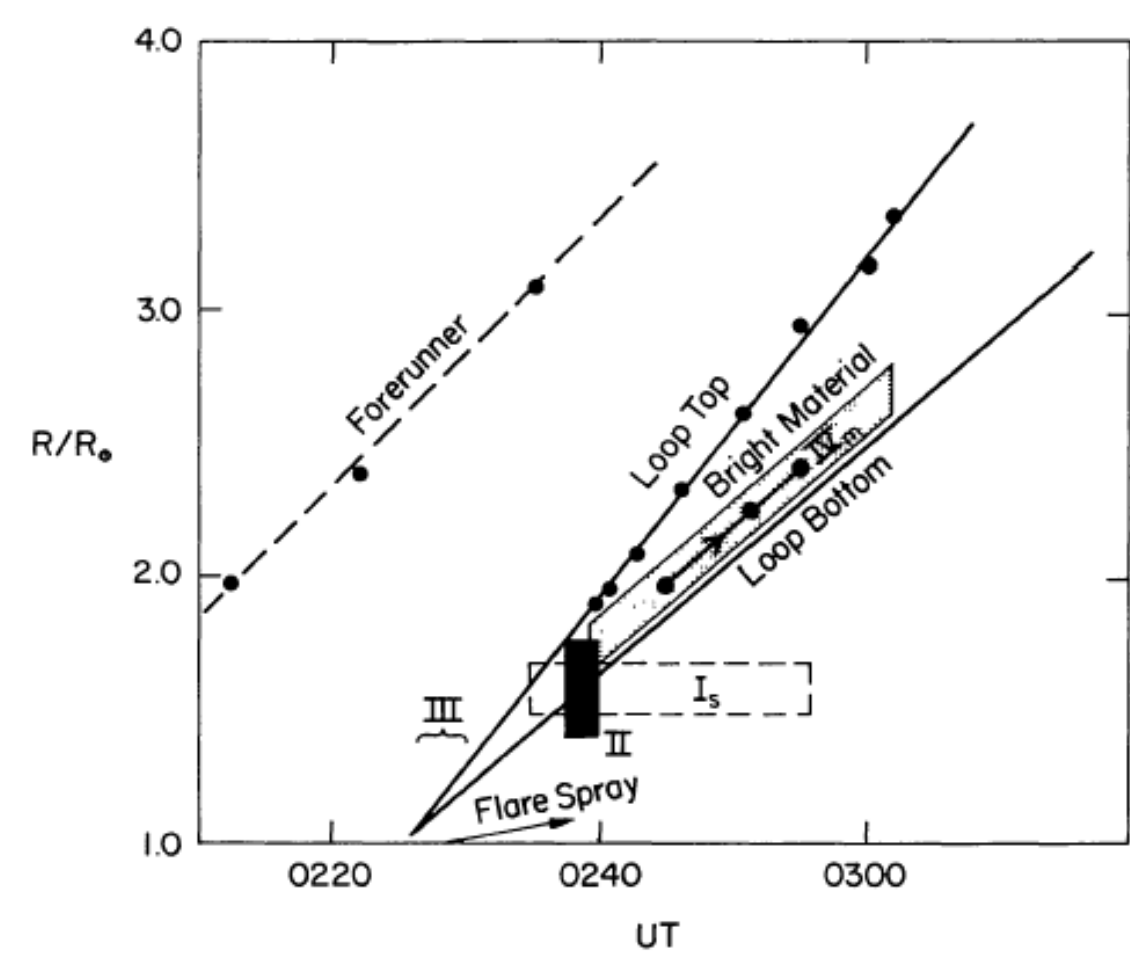


Fig. 1: Height-vs-time plots including an example of a moving type IV burst, interpreted as showing quasi-relativistic or relativistic electrons trapped in an expanding magnetic trap geometry (from Stewart *et al.*, 1982). This event, April 27, 1980, also exhibited a highly enhanced coronal density (some 30× model background) observable with a white-light coronagraph.

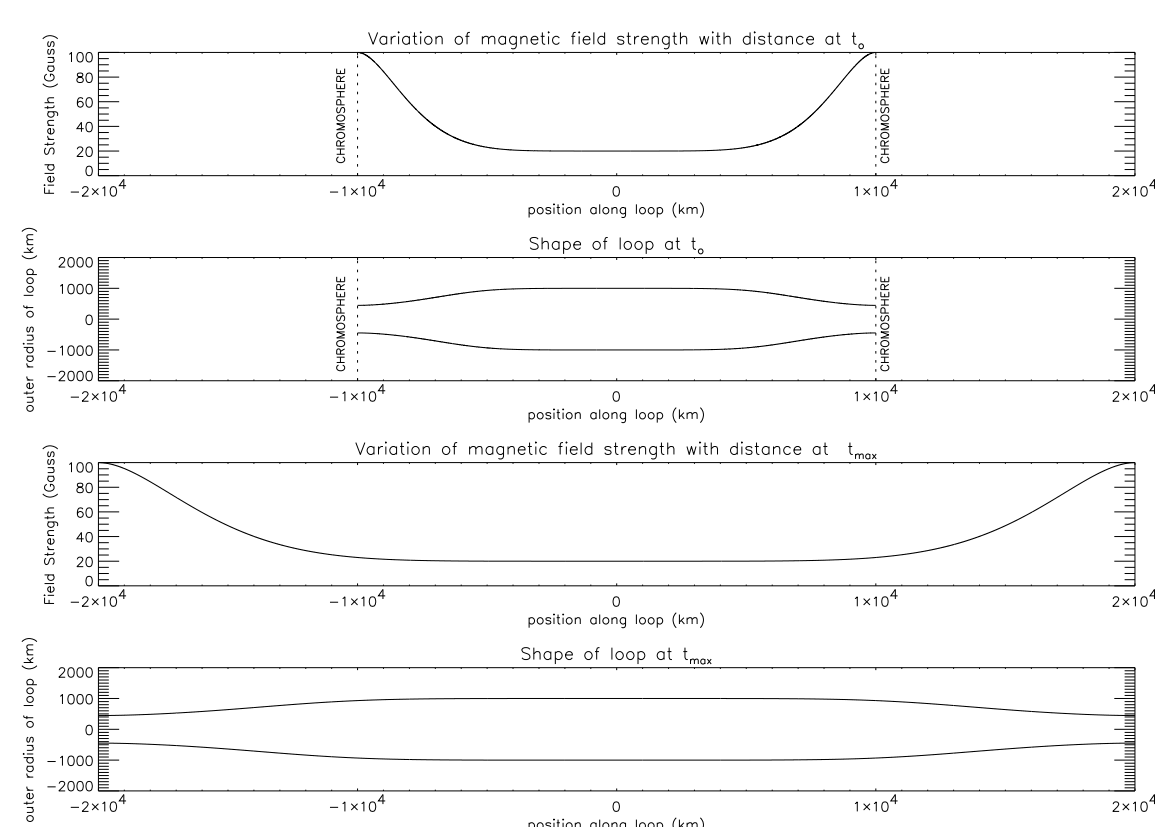


Fig. 3: Magnetic model in the geometry of MacKinnon and Brown (1990): Fixed magnetic field intensity B , loop length elongating with time. Note, the mathematical form of this field at any instant in time obeys $\nabla \cdot B = 0$

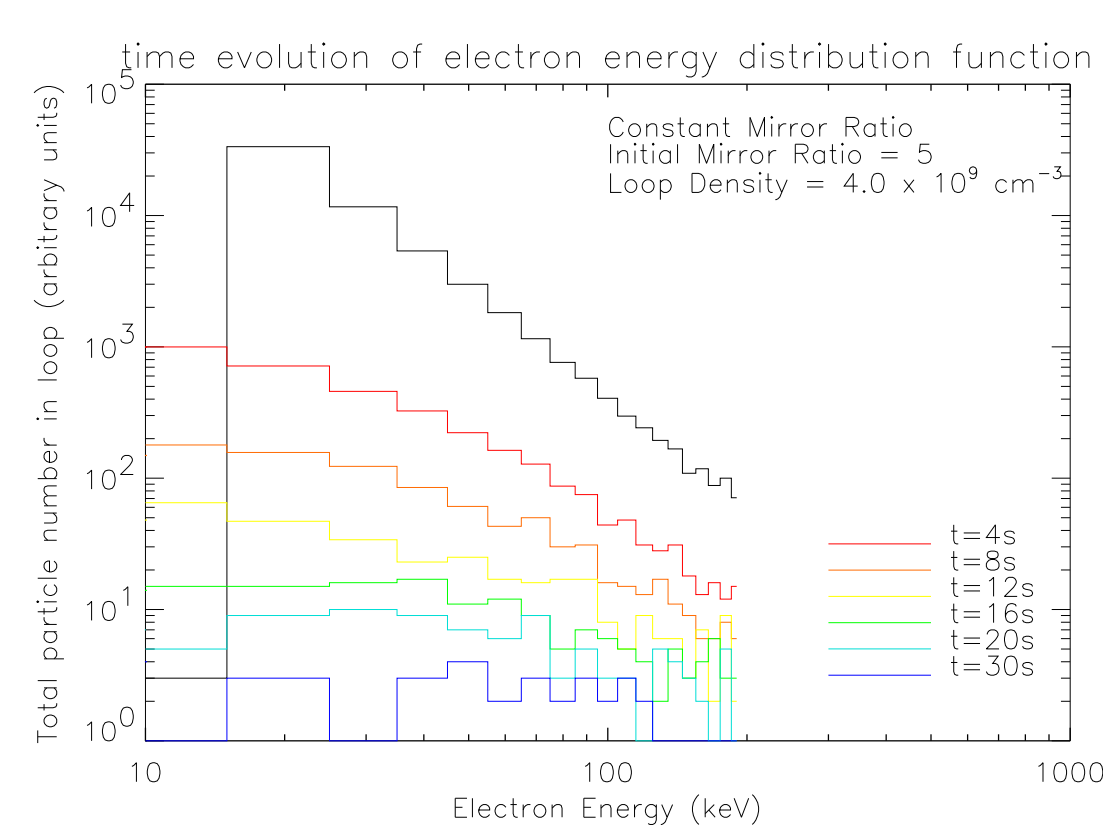


Fig. 5: Particle energy distributions color-coded by time, in time increments as indicated, for Model A (constant mirror ratio).

References

- Fletcher, L., *A&A* **326**, 1259 (1997).
 Fletcher, L., & Martens, P. C. H., *ApJ* **505**, 418 (1998).
 Hudson, H. S., Lin, R. P., and Stewart, R. T., *Solar Phys.* **75**, 245 (1982).
 Hudson, H. S., Kosugi, T., Nitta, N. V., & Shimojo, M. *ApJ* **561**, L211 (2001).
 MacKinnon, A. L., & Brown, J. C... *A&A* **232**, 544 (1990).
 Nitta, N. V., & Akiyama, S., *ApJ* **525**, L57 (1999).
 Stewart, R. T., *et al.*, *A&A* **116**, 217 (1982).
 Sturrock, P. A., *Plasma Physics* (Cambridge, the University Press), p. 19 (1994).

Introduction

Yohkoh soft X-ray observations have provided many examples of expanding loops originating in the core regions of solar flares and empirically linked (*e.g.* Nitta and Akiyama, 1999) with CMEs. Such structures presumably support phenomena observed at metric radio wavelengths, such as moving Type IV bursts (*e.g.*, Figure 1). These require relativistic electrons to be trapped in expanding magnetic structures. Now we have an example, shown in Figure 2, of a moving coronal hard X-ray source (from a behind-the-limb flare) suggesting the presence of quasi-relativistic electrons (20-50 keV) in a possibly similar environment (Hudson *et al.*, 2001).

Particle acceleration in solar flares occurs during the impulsive phase. Are the observations of the April 18, 2001 event consistent with the advection outwards of trapped particles resulting from this epoch, or is a further coronal particle acceleration required?

In this poster, we investigate numerically the evolution of a particle distribution trapped in an expanding magnetic loop. The inferred field motions during the expansions are slow relative to the particle transit times through them, so that the first and second adiabatic invariants hold (*e.g.* Sturrock, 1994), and we can use the guiding centre approximation to study particle motion.

Adiabatic development of trapped plasma and particles

We envision a plasma trapped within an expanding magnetic flux surface. The particle velocity distribution function has a thermal core and a non-thermal tail extending to high energies. Densities of $4 \times 10^9 \text{cm}^{-3}$ - much in excess of normal coronal density models - may prevail in the thermal core of the distribution (Hudson *et al.*, 2001). The thermal plasma will evolve according to the normal adiabatic laws, and we incorporate a background density variation in our models as appropriate.

In this treatment the tail particles have been energized by an unspecified acceleration mechanism related to the impulsive phase of the flare, and remain partially trapped within the expanding plasmoid, by the magnetic mirror force. Coulomb scattering permits diffusion into the loss-cone as a means of particle precipitation; (*e.g.* Fletcher, 1997) otherwise only cross-field drift motions or magnetic reconnection would permit particle escape.

The continuity equation for the evolving distribution function $f(v, \mu, S, t)$ is

$$\frac{\partial f}{\partial t} + \mu v \frac{\partial f}{\partial s} - D_{\mu\mu} \frac{\partial}{\partial v} \left(\frac{f}{v^2} \right) - \frac{D_{\mu\mu}}{v^3} \frac{\partial}{\partial \mu} \left[(1 - \mu^2) \frac{\partial f}{\partial \mu} \right] - \frac{v}{2} \frac{\partial}{\partial \mu} \left[(1 - \mu^2) \frac{d \ln B}{dS} f \right] + \frac{\dot{B}}{2B} \left(v \frac{\partial f}{\partial v} - \mu \frac{\partial f}{\partial \mu} \right) = 0$$

where v and μ are the particle speed and pitch angle, S is the co-ordinate along the magnetic field, $B(s, t)$ is the magnetic field strength and $D_{\mu\mu}$ is the Coulomb diffusion coefficient. We consider a model of expanding loops, following the geometry of MacKinnon and Brown (1992) as illustrated in Figures 3 and 4. We use stochastic simulation of test-particle trajectories (*e.g.* Fletcher, 1997) to permit scattering and field variations to be handled simultaneously. The detailed geometry of the expanding corona at the onset of a coronal mass ejection is not understood well at present, and so we make two simplifying assumptions for the first models. In Model A the loop elongates without change of field intensity B ; in Model B we allow B to decrease as the inverse square of the spatial scale. The number density of particles with which the high energy tail is colliding varies inversely with the volume of the loop.

Particles are followed from $t = 0$ in a loop which expands over the course of 100s. They are injected in a power-law in energy with index equal to 3, cutoff at 20 keV, and the spectrum extends up to 400 keV (limited for numerical reasons). Particles are initially assumed to be distributed uniformly along the loop. We follow the trapped-particle velocity distribution as a function of time; these particles determine the X-ray bremsstrahlung observed above the limb. Figures 5 and 6 show the time evolution of the spatially-integrated particle distribution function for the trapped electrons in each of these models.

Conclusions

For both models (elongating loop at fixed B and expanding loop with decreasing B) we find a rapid flattening of the input spectrum. This is accompanied in each case by large reductions in particle number. The reductions are higher than are found in simulations without loop/field expansion, since 'betatron deceleration' by the expanding field (since v_{\perp}^2/B is constant) provides an adiabatic focussing which, when coupled with the relatively high level of collisions taking particles across the loss-cone boundary enhances particle precipitation rates. Whereas the flat spectrum would be consistent with some of the over-the-limb hard X-ray observations, and in particular with the event of April 18, 2001, the brightness decrease seems to be in conflict with the observed event duration of about one minute, using the ambient density inferred by the observers. This suggests the need for continued particle acceleration, rather than a single acceleration epoch that happens prior to the field expansion into the corona.

Our technique of stochastic simulation provides a good approach for modeling the evolution of coronal hard X-ray sources. We intend to extend these calculations, for example to characterize the spatial distribution of the hard X-ray emission. The problem at present is the limited knowledge of field geometry and source particle distributions. The observations thus far are few and noisy, in spite of their importance for our understanding of the physics of coronal mass ejections and solar energetic particle events.

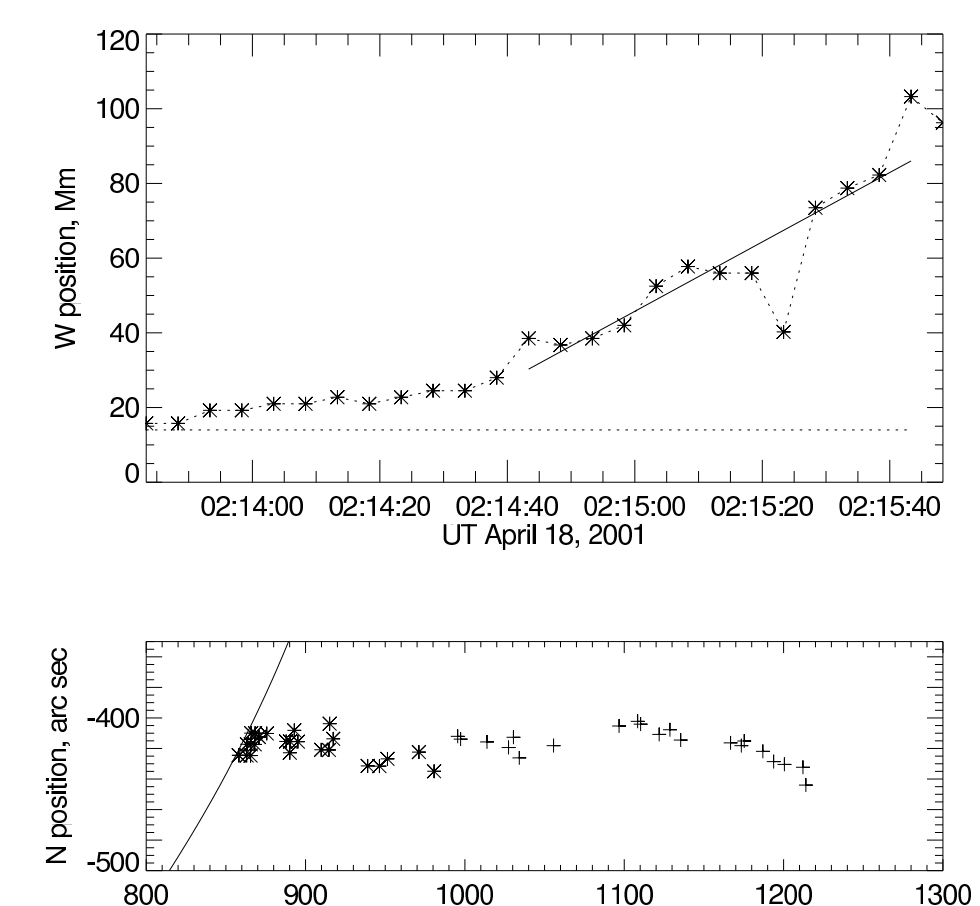


Fig. 2: Upper: Height vs. time for the moving coronal hard X-ray source observed by Hudson *et al.*, 2001. The points show the EW coordinates of the peak hard X-ray emission at 10-sec intervals, with the line indicating a projected velocity of about 1,000 km/s. Lower: Heliocentric positions of the hard X-ray source (*) and associated microwave source (+) at 5-sec intervals during the outward motion.

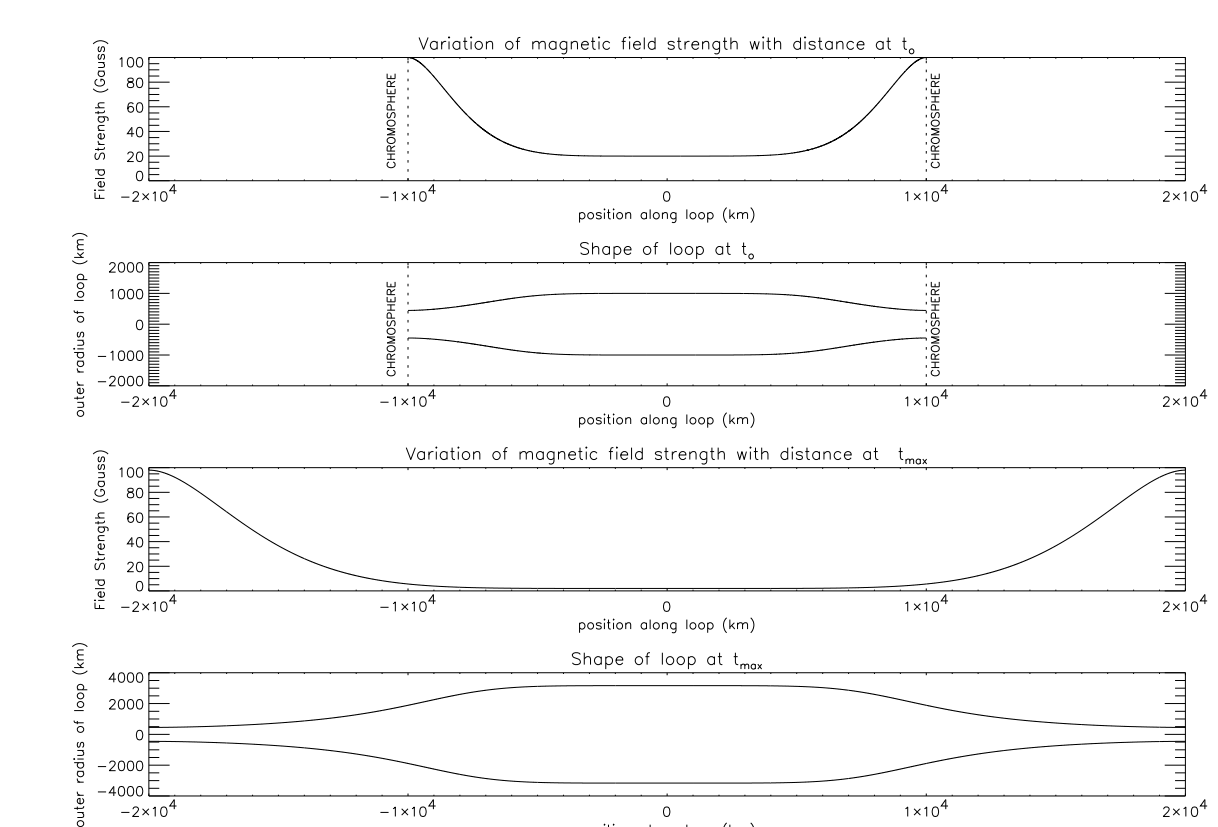


Fig. 4: Magnetic model for B diminishing with time in an isotropic expansion. As well as lengthening, the magnetic field at the apex of the loop decreases linearly with time. The background number density of particles in this loop decreases linearly with time, as the loop volume increases, but is assumed to remain uniformly distributed through the volume.

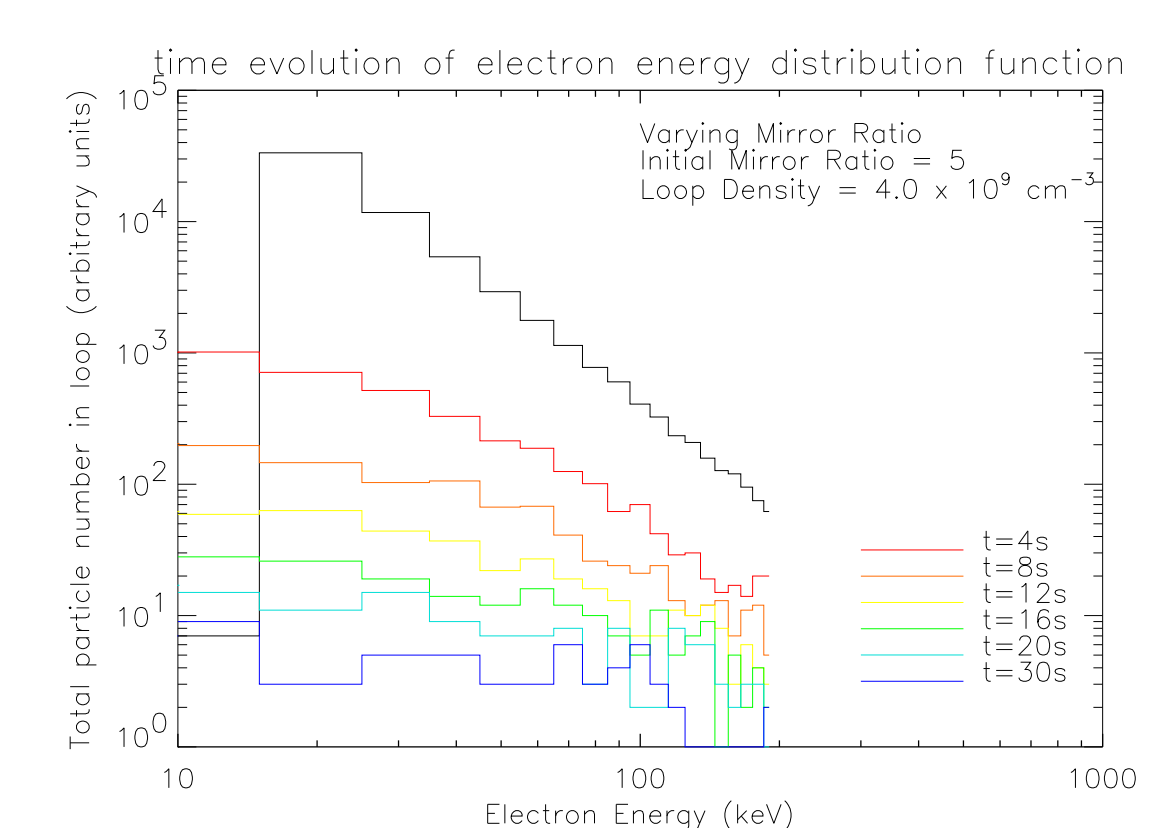


Fig. 6: Particle energy distributions color-coded by time, in time increments as indicated, for Model B (increasing mirror ratio). Compared to the distributions shown in Fig. 5, the particle losses as a function of time are not so great. The competing effects on particle population are (a) the varying magnetic field which leads to increased adiabatic focussing but also a decrease in the loss-cone volume and (b) the decreasing collisional density, which leads to decreased energy losses.

The similarity with Fig 5. indicates that, at least in the early phases of the event, the collisional losses are more important in determining the evolution of the population than is the magnetic field variation. Despite the fact that within the first 10 seconds the loss-cone volume decreases by 40%, the trapped population remains virtually the same.